Proceedings of the ASME 2010 3rd Joint US-European Fluids Engineering Summer Meeting and 8th International Conference on Nanochannels, Microchannels, and Minichannels
FEDSM-ICNMM2010
August 1-5, 2010, Montreal, Canada

FEDSM-ICNMM2010-31168

IR-Thermography and High speed imaging of Cerium Nitrate Precursor Droplets Heated by Monochromatic Irradiation

Abhishek Saha **Erick Tijerino** **Ranganathan Kumar** **Saptarshi Basu**

Mechanical, Materials and Aerospace Engineering Department
University of Central Florida, Orlando, FL 32816

Abstract:

An experimental setup using radiative heating has been used to understand the thermophysical phenomena and chemical transformations inside acoustically levitated cerium nitrate precursor droplets. IR imaging in conjunction with high speed imaging shows presence of four distinct phases of heating. The droplet initially undergoes pure vaporization followed by surface precipitation. This results in a gelatinous phase due to precipitation of cerium nitrate which eventually goes though chemical transformation and forms a porous precipitate. Transmission Electron Microscopy (TEM) of the final precipitate revealed the presence of trapped gases in the form of bubbles. TEM also showed the presence of nano-ceria crystalline structures at 70^{O}C. The current study also looks into the effect of different heating power on the process. At higher power each phase is sustained for smaller duration and higher maximum temperature. At all laser power, TEM showed the formation of nanoceria. In addition, the porosity of the final precipitate increased with power.

Introduction:

Ceria is widely used in solid oxide fuel cells, catalytic convertor, oxidation resistive coating [1-5]. Recently, use of nano-ceria has been reported by many authors in different fields such as spray coating, oxygen gas sensors, and medical sciences [6-8] due to better thermal and mechanical properties. Nanoceria thin film is used in optoelectronics [9] and electrochemistry [7] also because of its wide bandgap and optical transparency. Among the different methods of preparing nano-ceria using cerium nitrate, solution precursor plasma spray and High velocity oxy-flame processes are very popular in coating industry [10-12]. The plasma spray process uses a very high temperature of 9000K. On the other hand in oxy-flame process gas temperature reaches around 2400K. Literature survey shows that in spray coating, the choice of solution precursors such as cerium acetate [13], cerium chloride [9], cerium nitrate [9, 14] have been used as source compounds. Literature shows that the thermal decomposition of cerium nitrate to produce ceria starts around temperatures 250 ^{o}C-500^{o}C [9, 13].

For its high heating rate CO_2 laser has been used in many material processing and medical science applications [15-17]. A tunable CO_2 laser can be used for simulating similar heating conditions in plasma (with high laser power) [14, 18] or combustors (with low laser power). Park and Armstrong [19] reported their numerical work on vaporizing droplet heated by monochromatic radiation. Their work considered pure liquid droplets heated by a 10.6 μm CO_2 laser. They discussed about two distinct heating regimes: slow and fast. Fast heating resulted in explosive vaporization of the droplet, due to hot spots. On the other hand the process of slow heating is dominated by thermal diffusion reducing the chances of explosive vaporization. Basu and Cetegen [18] showed that the vaporization rate of a thermally irradiated droplet decreases in the

presence of non-vaporizing species. Their work also revealed that lower heating rate will provide enough time for mass diffusion within the droplet. This leads to gradual increase in concentration from the droplet center to its surface. But higher heating rate will result in sharp concentration gradients due to faster vaporization.

A few papers [19-21] have addressed vaporization characteristics and effect of acoustic waves on the evaporation rate of a single levitated droplet. It is generally accepted in the scientific community that acoustic levitation can be used to investigate different physical phenomena in a suspended droplet [16]. Yarin et al [20] reported an analytical work on levitated droplet vaporization rate. They mathematically showed that strong acoustic field has an effect on droplet shape (aspect ratio) which affects the natural vaporization process. The effect of acoustic streaming and droplet deformation was verified with experimental results. Tian and Apfel [21] studied vaporization of single and multiple droplets under acoustic streaming. Their experimental results also closely match results presented by Yarin [20]. However, all of these works have considered only pure evaporation of single component liquid droplet. Omrane et al [23] conducted a series of experiment of levitated liquid droplet. His experimental work was aided by optical diagnostics in the form of Laser Induced Florescence and Laser Induced Phosphorescence to measure the species concentration and temperature of the droplet. Their experiment was conducted with natural vaporization in the absence of any external heating source. By measuring concentration and temperature using florescence and phosphorescence, they demonstrated a new way of measuring two parameters simultaneously.

Current work uses high speed imaging and IR-thermography for in-situ optical diagnostics on a cerium nitrate droplet heated by a tunable CO_2 laser. The goal of the study is to determine different phases of heating. The current study is also aimed at understanding the effect of laser power on the vaporization process and final precipitate.

Experimental Set up

The experimental set up uses an ultrasonic levitator (Tec5 ultrasonic levitator, 100 kHz) to suspend the droplet. The suspended droplet was heated by a CO_2 laser radiating at 10.6 µm with a beam diameter of 2mm. The power of the laser can be tuned from 0 W to 30 W (~10MW/m^2) using a controller attached to the power supply. An IR camera was placed perpendicular to the laser beam to measure the temperature of the droplet. The IR camera (FLIR Silver: calibrated for a range of -5 to 200^{o}C with an accuracy of +/- 1^{o}C) was attached to a microscopic zoom (FLIR G3-F/2) lens to facilitate 3X magnification with a working distance of 40 mm. The IR camera was operated at 100 fps and the recorded images were processed by 'ALTAIR' software to extract the temperature data of the droplet during heating process. The integration time of the IR camera depends on the temperature range adapted. Most of the experiments were performed with a temperature range of 20-80^{o}C which needed an integration time of 1.63 msec. The camera is precalibrated for standard emissivity of 1. However, the emissivity can be changed using the ALTAIR software.

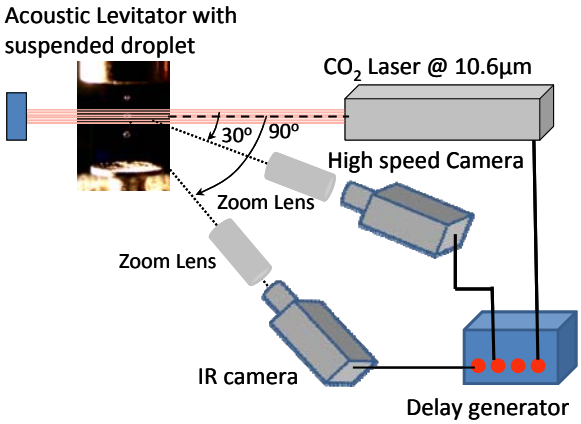

Figure 1: Experimental setup.

A high speed camera (Fastec TSHRMM, with maximum speed of 16000 frames per second) along with a zoom lens assembly (Navitar 6000) was used to capture the physical processes within the droplet during laser irradiation. This camera was placed at an angle of 30^o to the laser axis as shown in Figure 1. The event was

recorded at 1000 fps, without loss of spatial resolution. The images from the high speed camera were used to determine the instantaneous diameter of the droplet as it is faster than the IR camera (100 fps). To facilitate fine adjustment of the relative position, the IR camera was placed on an X-Y stage while the levitator was attached to an X-Y-Z stage. The high speed camera was also positioned on a uni-directional stage (X-stage). The laser and the cameras were synchronized using an external delay generator.

In this work, 0.576M cerium nitrate aqueous solution was used to generate the droplet. The solution was prepared by dissolving 99% pure Cerium Nitrate hexa-hydrate salt into DI water with the help of a magnetic stirrer and acoustic sonication. The droplets were generated and deployed to the pressure node of the levitator by a micro needle. For every run of the experiment initial diameter of the droplet was maintained at 500 μm (+/- 30 μm). The droplet was heated with the laser at different power levels until phase transformation and morphological changes were complete.

After the experiment, the IR and high speed images were analyzed to obtain the temperature and diameter data. The temperature data was obtained by defining a zone of interest around the surface of the droplet in each IR image, and the maximum, minimum, average and standard deviation of the temperature within the droplet were calculated. It is important to mention that the droplet sometimes oscillated from side to side with respect to the IR camera axis during the experiment which resulted in and out of focus images. The out of focus images were not considered for analysis.

The high speed images with higher temporal resolution were used to calculate the diameter of the droplet using Motion Measure software. To calculate the instantaneous diameter, an edge around the droplet was defined. An equivalent diameter was calculated from the area under the curve (edge).

The final form of the precipitate was collected on copper grids to perform ex-situ analyses. The samples were analyzed using optical microscope, scanning electron microscopy (SEM) and transmission electron microscopy (TEM) in order to understand the microstructure and crystallography of the samples.

Result and Discussions

The experiment was performed for three different heating power levels, High power (1.8 MW/m^2), medium power (1.3 MW/m^2) and low power (0.75 MW/m^2).

High Laser Power (1.8 MW/m^2):

The analysis of high speed and IR images showed that the droplet undergoes at least four distinct phases during the heating process. In general, the droplet vaporizes and distorts to a bowl-shape as it precipitates. At this point, chemical reaction takes places that converts cerium nitrate to nanoceria. The total heating process for this condition is of 5.3sec. Each phase is described in the following paragraphs in detail.

Figure 2 shows the diameter change for 30% laser power. The figure marks all the four phases of heating. Initial phase is termed as 'pure evaporation', which is dominated by evaporation of water from the droplet. Figure 3 shows the temperature evolution during the heating process. Initially, mean temperature rises and eventually attains a steady value (figure 3a). Figure 3b shows a higher standard deviation of the temperature in the initial phase of this heating regime. It can be attributed to the directional nature of radiative heating used in the current experiment. The droplet shows a non-uniform temperature distribution for some time with the heating side expectedly exposed to a higher temperature. The temperature front moves across the droplet and eventually in 0.8 sec the surface temperature becomes uniform. The later part in the pure evaporation phase is marked by smaller differences in maximum and average temperature and lower standard deviation. At the end of this phase, the maximum and average temperatures are 68^oC and 66^oC respectively. The diameter reduction plot (figure 2) shows almost a constant slope in this phase, with the diameter reaching 76% of the initial value. Simple convective evaporation is generally characterized by D^2 law which is marked by the parabolic nature of diameter reduction curve with time. However, D^2 law assumes uniform surface temperature of the droplet of pure liquid (no solute present). The

current experiment satisfied none of these conditions as it deviated from D^2 law.

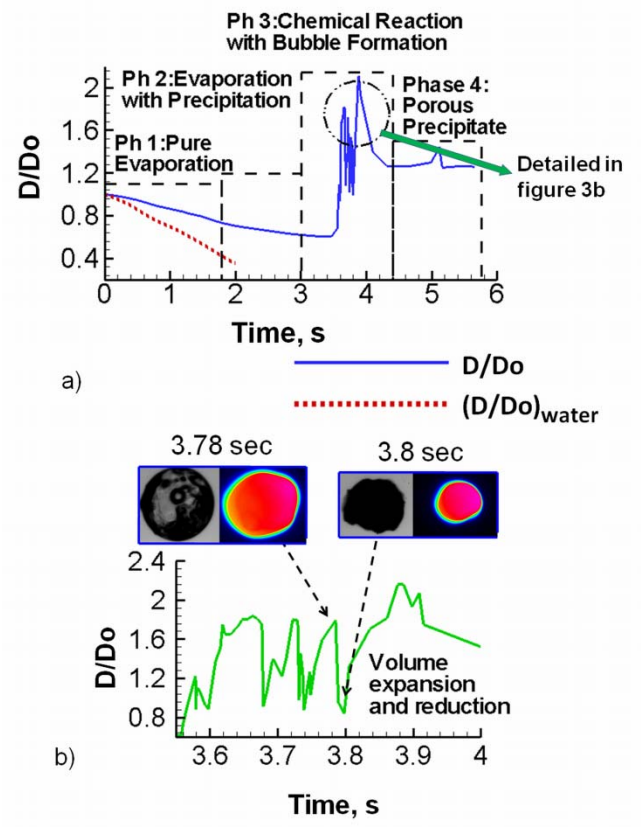

Figure 2: a) Evolution of diameter with time at high laser power (1.8 MW/m^2) for cerium nitrate and water b) expanded view of phase 3: chemical reaction and bubble formation.

The next phase of the heating process termed as evaporation with precipitation is characterized by a slower rate of evaporation. The onset of this region is marked by the triggering of surface precipitation, resulting in slower diameter reduction rate. Precipitation reduces the droplet to a bowl shape. Detailed observation of high speed images shows the formation of precipitate around the droplet. Due to substantial evaporation of water, the solute concentration increases to super saturation limit. This triggers the precipitation mechanism near the surface of the droplet where evaporation takes place. The rate of evaporation which is governed by Raoult's law slows down due to the presence of solid precipitate. For single vaporizing species,

$$P' = x_{solv}.P_{solv}$$

P' = *effective vapor pressure*

x_{solv} = *mole fraction of the vaporizing species*

P_{solv} = *vapor pressure*

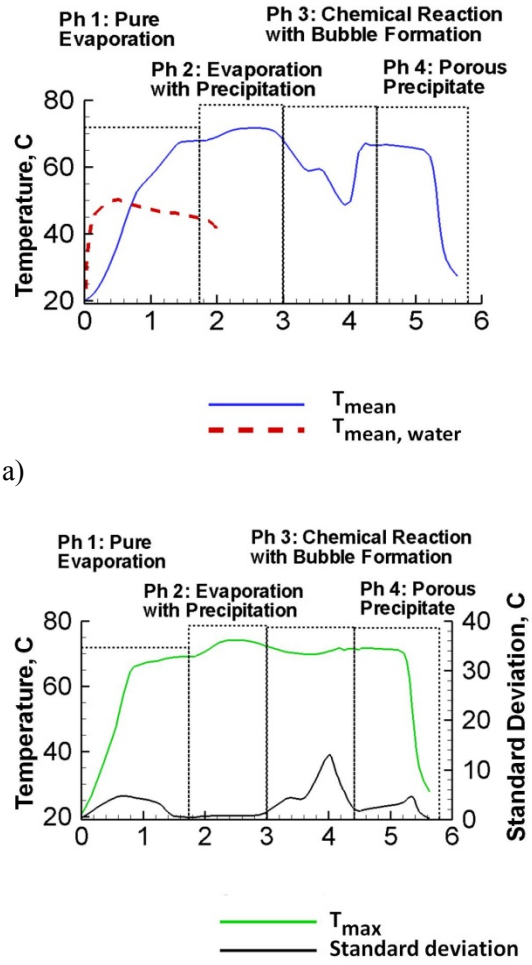

Figure 3: Temperature evolution with time

a) Mean temperature for cerium nitrate and water
b) Maximum temperature and standard deviation

Increase in solute concentration reduces mole fraction of the solvent (water here). Thus the vapor pressure decreases reducing the vaporization rate. This is marked by a decrease in slope of diameter in this region of evaporation with precipitation shown in Figure 2a. Slower evaporation requires less latent heat which increases the amount of sensible heat and thus

the droplet temperature increase with time in this region of heating. Figure 3b shows surface temperature reaches a maximum of 75^{O}C. The surface temperature of the droplet remains almost uniform on the surface, which can be inferred from the lower standard deviation of surface temperature. This zone of heating extends for 1.2 sec reducing the diameter to 60% of initial value.

Next phase of heating is distinctly marked by bubble formation and expansion of the droplet. This zone is termed as chemical reaction and bubble formation. High speed images clearly show erratic bubbling and collapsing phenomena. This bubble formation is due to thermal decomposition of cerium nitrate, which results in ceria and nitrogen oxides. Gases liberated as products of chemical reaction emanate from the droplet in the form of bubbles. Nitrogen dioxide and oxygen created as byproducts of chemical reaction are manifested by the formation of bubbles. These bubbles result in sudden expansion of the droplet like a balloon, and are subsequently vented out through the pores. This process of ballooning and collapsing is repeated throughout the entire phase, showing rapid oscillations in droplet diameter (Figure 2b) for 0.4s, ranging from 100% to 200% of its original diameter. The IR images show a non-uniform temperature distribution of droplet surface temperature. There is a wide difference in maximum and average surface temperature. Although the maximum droplet temperature remains around 70^{o}C (figure 3b), the average temperature (figure 3a) goes as low as 50^{o}C. Since the bubbles are low temperature zones in the droplet, the average temperature goes down, increasing the standard deviation to as high as 15^{o}C (figure 3b). as. This phase of chemical transformation goes for 1.1 sec resulting in the formation of ceria from cerium nitrate.

The final phase of heating named as porous precipitate is very quiet in nature. This region does not show much change in diameter which proves the evaporation and chemical transformation have been completed in previous regimes of heating. Droplet diameter does not change with time except for very small bubble formations. The final diameter of the droplet is around 120% of its initial size due to porous microstructure. The venting of gases liberated during chemical transformation of cerium nitrate creates pores in the solid precipitate. This process of chemical transformation is so rapid that some of the gases might have been trapped as submerged bubbles within the precipitate. Both the mean and maximum temperature (figure 3a and b) plot in this phase of heating shows almost a constant trend until the laser was turned off. After that the temperature drops down very sharply. Some portions of the droplet cool down faster than others resulting in a high standard deviation of surface temperature (figure 3b).

Table 1 shows sample high speed and IR images at different phases of the heating process.

	Ph 1: Pure Evap.	Ph 2: Evap. With Precip.	Ph 3: Chemical Reaction and Bubble Formation			Ph 4: Porous Precip.
	1.53 s	2.54 s	3.65 s	3.78 s	3.8 s	5.25 s
High Speed Image	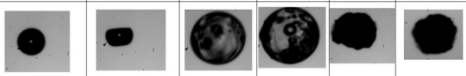					
IR images	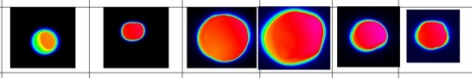					
D/Do	0.8	0.7	1.7	1.8	0.8	1.2
Mean Temp, C	68	72	54	49	52	66
Std dev, C	0.4	0.8	5.3	7.9	6.2	2.1

Table 1: Different phases of heating process for high power (1.8 MW/m^2)

A separate experiment was performed with water droplet. In figure 2a and 3a show the diameter and temperature plots for water droplet. Clearly the water droplet vaporizes much faster than cerium nitrate droplet. As explained earlier presence of solute results in a decrease in vapor pressure of the solvent, which in turn reduces surface vaporization. Faster evaporation of pure water requires more latent heat reducing available sensible heat for the droplet. This results in lower temperature rise in the case of pure water.

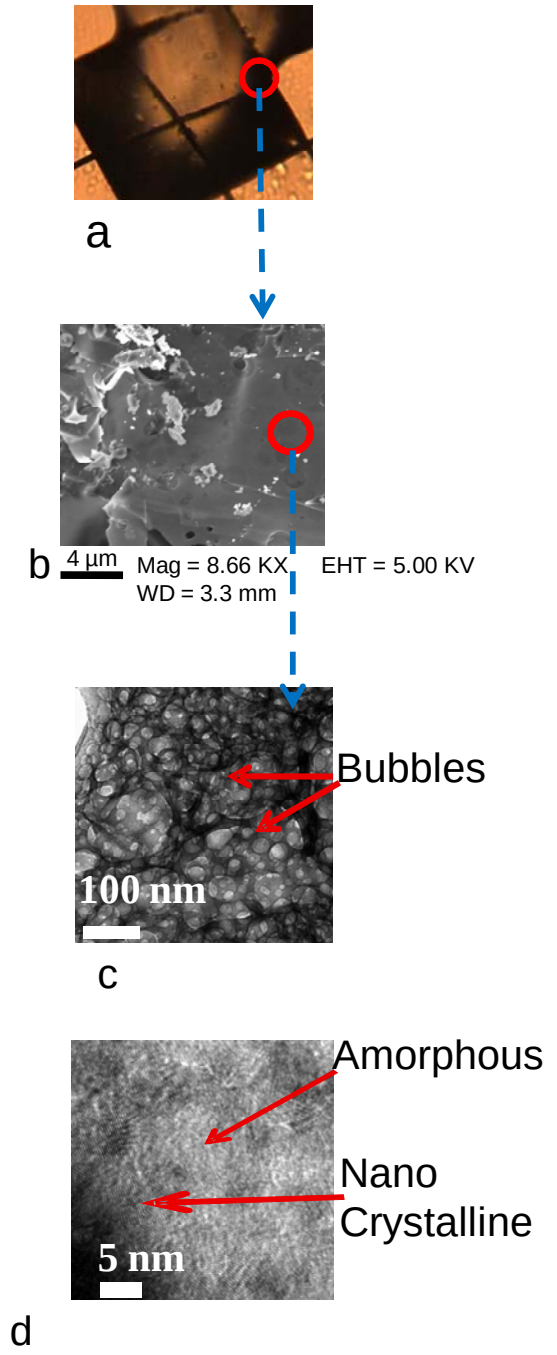

Figure 4: Final precipitate a)under optical microscope, b) Scanning electron microscope, c) Transmission electron microscope

The ex-situ analysis revealed some interesting finding of the precipitate. Figure 4 shows results from ex-situ analysis. Under optical microscope the precipitate looked optically translucent as shown in figure 4a. SEM results showed the presence of a smooth layer which is partially optical clear. As shown in figure 4c and 4d, TEM images confirmed presence of trapped gases in the form of bubbles inside the microstructure. Also TEM images showed co-existence of crystalline and amorphous phases within the precipitate. The amorphous phases are responsible for the translucent nature of the precipitate. TEM images also revealed that the crystalline phase has a grain size of around 5-10 nm, confirming the formation of nano-particles. EDX revealed that the primary two elements present in the precipitates are cerium and oxygen with atomic and mass percentage very close to CeO_2. Thus it could be inferred that cerium nitrate was transformed into nano-ceria.

Low Laser Power (0.75 MW/m^2):

All the four phases of the heating process described in the previous section can also be observed in the case of low power with a heating flux of 0.75 MW/m^2. However, the total time of heating is much longer (23.2s) compared to the high laser power. Figures 5 and 6 show the diameter and temperature plots for low power condition.

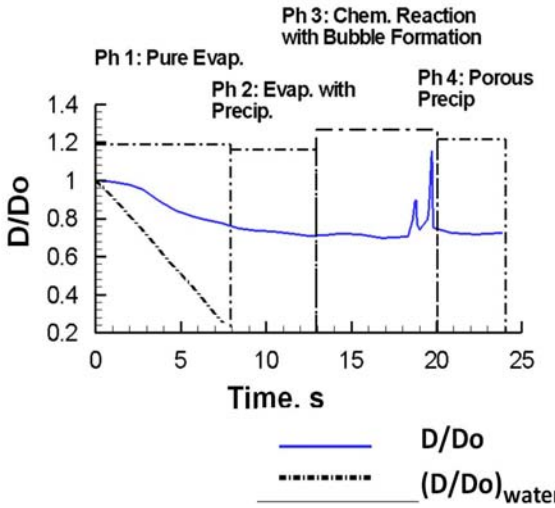

Figure 5: Diameter evolution for cerium nitrate and water for low power (0.75 MW/m^2).

The pure evaporation phase is extended to 8 sec with a sharp rise in temperature at initial stages. The mean temperature reaches around 55^{o}C and becomes almost constant (figure 6a). Figure 6b shows that the maximum temperature follows the same trend and saturates around 58^{o}C. As in the case of high power heating, initial phase of

heating process shows a higher standard deviation of the droplet surface temperature (figure 6b). As explained earlier, this can be attributed to the directional nature of the heating process. The diameter plot in figure 5 shows a slower vaporization rate for initial phase of 2.5 sec.

The second phase of heating 'evaporation with precipitation' is very similar with case of high heating power (1.8 MW/m^2) with slow vaporizing rate and uniform surface temperature around the droplet. The slope change between the first and second phases is discernable as in high power.

The phase of 'chemical reaction and bubble formation' in the case of low (0.75 MW/m^2) laser power is not very erratic in nature as in high (1.8 MW/m^2) laser power. The primary reason is that the amount of irradiative heat dumped into the droplet is low and hence the thermal decomposition of cerium nitrate is slow in progression. The droplet expands slightly as seen in the diameter plot of figure 5 towards the end of this phase. The temperature remains constant around 55-57^{o}C. At the end of this phase at 20s the droplet completely transforms into a solid particle.

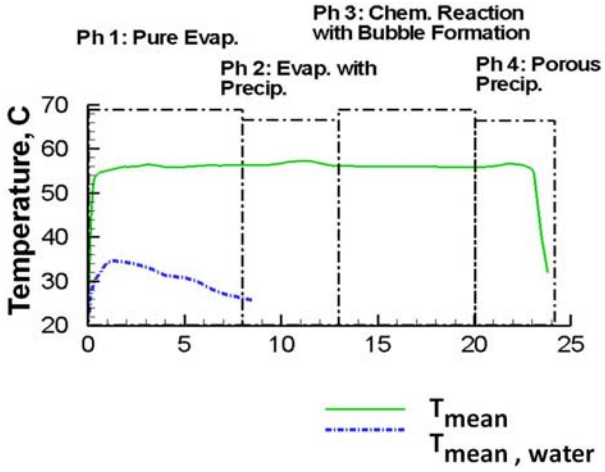

a)

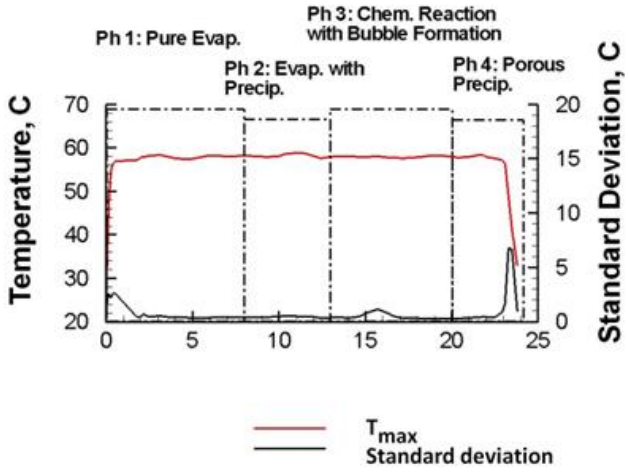

b)

Figure 6: Temperature evolution for low laser power a) T_{mean} for cerium nitrate and water. b) T_{max} and std dev for cerium nitrate

As in the case of high laser power, with lower power also the last phase of porous precipitate is calm. Table 2 shows the different phases for low power along with representative images, drop size and temperature in each phase.

Table 2 shows different phases of heating with low heating power (1.8 MW/m^2).

	Ph 1: Pure Evap.	Ph 2: Evap. With Precip.	Ph 3: Chemical Reaction and Bubble Formation			Ph 4: Porous Precip.
	5.15 s	11.5 s	18.5 s	19.0 s	19.8 s	22.0 s
High Speed Image	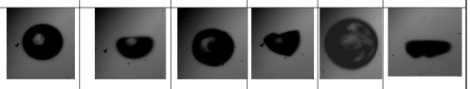					
IR images	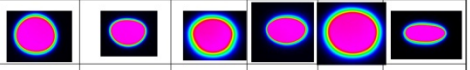					
D/Do	0.82	0.75	0.87	0.78	1.1	0.8
Mean Temp, C	56.1	59.2	56.2	56.4	52	56.26
Std dev, C	0.3	0.66	0.29	0.33	0.35	0.41

Table 2: Different phases of heating process for low power (3W)

The ex-situ analyses with TEM showed similar results. TEM images show that final precipitate contained both nano-crystalline and amorphous structure. Also the primary element present in

the microstructure was found out to be cerium and oxygen, forming nanoceria.
A separate experiment was conducted with pure water which shows faster evaporation and lower temperature rise compared to cerium nitrate solution as shown in figure 5 and figure 6. As described before this can be explained by Raoult's law. As seen before, the presence of cerium nitrate reduces the vaporization rate allowing more sensible heat for the droplet to increase in temperature.

Medium Laser Power (1.3 MW/m^2):

An experiment was conducted with medium laser power (1.3 MW/m^2) as well. Predictably, high speed and IR images clearly indicate that the result for this case falls between two extreme cases marked by low (0.75 MW/m^2) and high laser power (1.8 MW/m^2). The maximum temperature of the droplet reaches 72^oC.

Porosity Calculation:

The TEM analysis of final microstructure for both high and low power cases were found to contain bubbles. Thus, the final precipitates for all laser power are porous in nature. A conservative analysis was performed to quantify the porosity of the final microstructure.
The mass of ceria was calculated assuming the chemical reaction to be complete. This was used to find out the theoretical volume of the precipitate using standard density of ceria. The actual volume of the precipitate was calculated by using high speed images. , and the percentage of porosity is defined as,

$$\%\ of\ Porosity = \frac{actual\ volume - theoretical\ volume}{actual\ volume} x100$$

The percent of porosity for three different power levels is plotted in Figure 7.

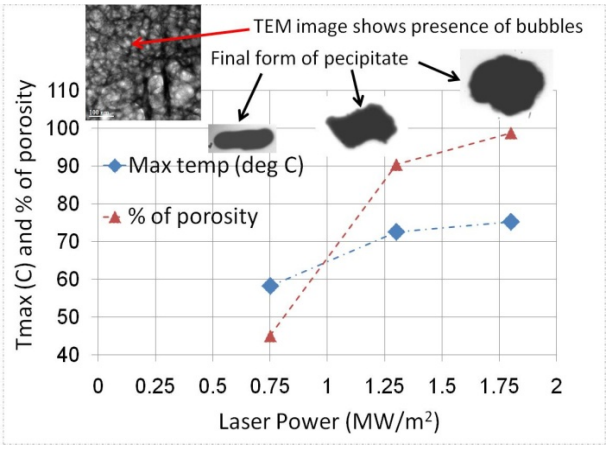

Figure 7: Porosity of final precipitate with maximum temperature for different laser power.

The plot shows that the porosity increases with laser power. It follows the same trend with the maximum temperature of the droplet. The porosity is a result of trapped gases liberated during the chemical reaction. With increase in heating power the reaction time scale also reduces or in other words, the gases are released much faster. This increases the amount of trapped gases thus increasing the porosity.

Conclusion:

This paper shows decomposition of cerium nitrate into nanoceria particles at low temperatures when a droplet is levitated and radiatively heated by a CO_2 laser. Four distinct phases have been delineated and the heat transfer process in each is discussed. Through high speed and IR imaging clearly show the distinction in the first two phases of pure vaporization and precipitate formation. The third volatile phase where the chemical reaction is slightly over a second is the highlight of this work. This phase is marked by the formation of nanoceria and nitrogen oxides; the formation of gases causes expansion of the droplet and its release through the pores contraction. This remarkable oscillatory behavior is captured for each of the laser power, albeit at different frequencies. Due to these pores, the final precipitate contains porous microstructure, and was confirmed by TEM Images. The effect of laser power in distinguishing the phases was quantified but predictable. The maximum

temperature of the droplet increases with power, and the time scale for chemical reaction is lower, and explains the high porosity for higher laser power.

References:

[1] B. C. H. Steele, Solid State Ionics 12, 391 (1984)
[2] M. Mogensen, N. M. Sammes, and G. A. Tompsett, Solid State Ionics 129, 63 (2000)
[3] A. Tschope, D. Schaadt, R. Birringer, and J. Y. Ying, Nanostruct. Mater. 9, 423 (1997)
[4] L. Tye and N. A. El-Masry, Appl. Phys. Lett. 65, 3081 (1994)
[5] S. Seal, S. K. Roy, S. K. Bose, and S. C. Kuiry, J. Mater., 52 [1–8] (2000)
[6] S. Patil, S.C. Kuiry, S. Seal and R. Vanfleet, Journal of Nanoparticle Research 4 (2002), pages 433–438.
[7] W. C. Maskell and B. C. H. Steele, Journal Journal of Applied Electrochemistry 16, 4, 1986
[8] R. W. Tarnuzzer, J Colon,S Patil and S Seal, Nano Letters 5, 12 (2005)
[9] B. Elidrissi, M. Addou, M. Regragui, C. Monty, A. Bougrine and A. kachouane, Thin Solid Films, 379, 23, 2000.
[10] A. Agarwal, T. Mckechnie, and S. Seal, J. Therm. Spray Technol., 12, 3, (2003)
[11] E. Brinley, K. S. Babu and S. Seal, Journal of the Minerals, Metals and Materials Society 59, 7 (2007)
[12] V. Viswanathan, R. Filmalter, S. Patil, S. Deshpande, and S. Seal, Journal of the American Ceramic Society, 90 (2007)
[13] A.I.Y. Tok, F.Y.C. Boey, Z. Dong and X.L. Sun, J. Matls Proc Tech, 190, 217 (2007)
[14] A. Saha, V. Singh, S. Seal and S. Basu, Surface and Coatings Technology 203, 15, (2009)
[15] S H Zhang, J H Yoon, M X Li, T Y Cho, Y K Joo and J Y Cho, Materials Chemistry and Physics 119, 3, (2010)
[16] K. Chen, B.Z. Chang, M. Ju, X.H. Zhang and H. Gu, British Journal of Dermatology 156 3, (2006)
[17] G Dedigamuwa, P Mukherjee, H Srikant, S Witanachchi, Chemical Engineering and Science Proceedings, 28, 6, (2008)
[18] S Basu, B M. Cetegen, Journal of Heat Transfer, 130, 7 (2008)
[19] B S Park and R L Armstrong, Applied Optics, Vol. 28, No. 17
[20] A Yarin, M Pfaffenlehner, C Tropea, Journal of Fluid Mechanics 356, (1998).
[21] Y. Tian, R. Apfel, Journal of Aerosol Science 27, (1996).
[22] E. Wulsten, G Lee, Chemical Engineering Science 63 (2008)
[23] A. Omrane, S. Santesson, M. Aldéna and S. Nilsson, Lab Chip, 4 , 291, (2004)